DEUTSCHES ELEKTRONEN – SYNCHROTRON

DESY 91-085
August 1991

Associate $J/\psi + \gamma$ Production: A Clean Probe of Gluon Densities

M. Drees

Deutsches Elektronen-Synchrotron DESY, Hamburg

C.S. Kim

Dept. of Physics, Univ. of Durham, England, U.K.

ISSN 0418-9833

NOTKESTRASSE 85 · D-2000 HAMBURG 52

DESY 91-085
August 1991

ISSN 0418-9833

Associate $J/\psi + \gamma$ Production: A Clean Probe of Gluon Densities

Manuel Drees
Theorie-Gruppe, DESY, Notkestr. 85, D2000 Hamburg 52, Germany

C.S. Kim*
Dept. of Physics, Univ. of Durham, Durham DH1 3LE, England

Abstract

We discuss the associate production of a J/ψ meson and a photon at $p\bar{p}$ (or pp) and ep colliders. By requiring the J/ψ to decay into an e^+e^- or $\mu^+\mu^-$ pair, we end up with an exceptionally clean final state. Furthermore, in leading order it can only be produced via gluon fusion. This process can therefore serve as a very clean probe of the gluon densities inside the proton as well as the photon. Numerical results are presented for the Tevatron $p\bar{p}$ and HERA ep colliders.

---

*Address after September 1991: Gruppe theor. Hochenergiephysik, Abt. Physik, Univ. Dortmund, P.O. Box 500 500, D4600 Dortmund 50, Germany. Bitnet address: UPH089@DDOHRZ11

1. Introduction

The production of heavy $Q\overline{Q}$ bound states (quarkonia) offers a good testing ground for perturbative QCD, since here one combines relatively large cross sections with rather clean final states. The large cross sections are, of course, due to the strong (colour) interactions of the quarks Q; clean signals emerge when the s-wave vector states (J/ψ or Υ) decay into a pair of charged leptons (e^+e^- or $\mu^+\mu^-$). Unfortunately the theoretical analysis of the inclusive production of quarkonia in hadronic collisions is complicated, due to the large number of contributing processes. For instance, the following processes contribute [1] to hadro-production of J/ψ:

$$\begin{aligned} g + g &\rightarrow J/\psi + g; \\ g + g &\rightarrow \chi_i(\rightarrow J/\psi + \gamma) + g; \\ g + q &\rightarrow \chi_i(\rightarrow J/\psi + \gamma) + q; \\ q + \bar{q} &\rightarrow \chi_i(\rightarrow J/\psi + \gamma) + g; \\ g + g, q + \bar{q} &\rightarrow b(\rightarrow J/\psi + X) + \bar{b}. \end{aligned} \tag{1}$$

For the photo- (or lepto-) production of J/ψ, one has to consider the processes [2]

$$\begin{aligned} \gamma + g &\rightarrow J/\psi + g; \\ \gamma + g &\rightarrow b(\rightarrow J/\psi + X) + \bar{b}. \end{aligned} \tag{2}$$

At the relatively low energies of fixed target experiments, only the first reaction in Eq. (2) leads to a sizeable cross section. Indeed, recently the NMC collaboration has shown [3] that this reaction can be used to determine the large-x behaviour of the gluon distribution inside the proton. However, at the much higher energies that can be achieved at the upcoming HERA collider the situation is considerably more complicated; here one does not only have to include [4] J/ψ production from b decays, but also *all* processes of Eq. (1), since at these energies the quark and gluon content [5] of (quasi-)real photons can no longer be ignored. Indeed, J/ψ production at HERA has been suggested [6, 7] as a probe of the gluon content of the photon, about which very little experimental information exists to date.[1] At the same time, one hopes to constrain [9] the small-x behaviour of the gluon content of the *proton* using reactions (2). In order to achieve both goals, one will clearly have to discriminate between the different mechanisms of J/ψ production, and various methods to do this have been suggested [7].

Another staple of perturbative QCD is the production of direct photons in hadron-hadron collisions [10]; more recently, these calculations have also been extended to ep colliders [11]. In leading order, direct photons can be produced by gq scattering or $q\bar{q}$ annihilation, so the analysis of such events at high energy $p\bar{p}$ or ep colliders is again quite

---

[1] Recently the AMY collaboration has shown [8] that a nonzero gluon content of the photon is required by their data on jet production in $\gamma\gamma$ collisions; however, the present data do not constrain the gluon content of the photon very much.

complicated. The situation is simplified when one requires [12] a heavy c or b quark to be produced together with the photon, but these reactions are not well suited to measure gluon structure functions, since the cross sections also depend on the poorly understood heavy quark distribution functions. This difficulty is avoided if we move the second heavy quark from the initial to the final state; if we in addition require the two heavy quarks to form a bound state, we can expect a very clean final state, as discussed above. In this letter we therefore study the associate production of a $Q\overline{Q}$ bound state and a hard, isolated photon. We focus on the production of J/ψ states, which offer the largest rates, but the generalization to other s-wave $J = 1$ $c\bar{c}$ or $b\bar{b}$ states is straightforward.

In leading order the $J/\psi + \gamma$ final state can only be produced in gg fusion, see Fig. 1:

$$g + g \to J/\psi + \gamma; \tag{3a}$$

$$g + g \to \chi_c \to J/\psi + \gamma. \tag{3b}$$

The reaction (3b) can only produce photons with small transverse momentum p_T; since we are interested in the production of *isolated* photons with high p_T, we only need to consider reaction (3a). (Note that $g + g \to \chi_c + \gamma$ is not possible.) The cross section is then given by

$$d\sigma(A + B \to J/\psi + \gamma + X) = \int dx_1 dx_2 f_{g|A}(x_1) f_{g|B}(x_2) d\hat{\sigma}(g + g \to J/\psi + \gamma), \tag{4}$$

where A and B can be a hadron, photon, or electron. We will use the so-called colour singlet model to estimate the hard subprocess cross section $\hat{\sigma}$. In this model the J/ψ is treated as a nonrelativistic $c\bar{c}$ bound state. One then has [13]

$$\frac{d\hat{\sigma}(g + g \to J/\psi + \gamma)}{d\hat{t}} = \frac{16\pi\alpha\alpha_s^2 m_\psi |R(0)|^2}{27\hat{s}^2} \left[\frac{\hat{s}^2}{\left(\hat{t} - m_\psi^2\right)^2 \left(\hat{u} - m_\psi^2\right)^2} + \frac{\hat{t}^2}{\left(\hat{u} - m_\psi^2\right)^2 \left(\hat{s} - m_\psi^2\right)^2} + \frac{\hat{u}^2}{\left(\hat{s} - m_\psi^2\right)^2 \left(\hat{t} - m_\psi^2\right)^2} \right]; \tag{5}$$

here, $\hat{s}, \hat{t}$ and $\hat{u}$ are the Mandelstam variables of the parton-parton collision, $m_\psi = 3.1\ GeV$ is the mass of the J/ψ meson, and the $c\bar{c}$ wave function at the origin $|R(0)|^2$ can be determined from the leptonic decay width of J/ψ:

$$\Gamma(J/\psi \to e^+e^-) = \frac{16\alpha^2}{9m_\psi^2} |R(0)|^2 = 4.72\ keV \Rightarrow |R(0)|^2 = 0.48\ GeV^3. \tag{6}$$

Since higher order QCD corrections to Eq. (5) have not yet been computed, we use leading order expressions everywhere; we will also stick to leading order structure functions when evaluating Eq. (4). The NMC collaboration found [3] that this leading order formalism describes the shape of all kinematical distributions quite well, while the prediction for

the normalization of the signal was too small by a factor of 2.4, even though the QCD corrected version of Eq. (6) was used, which increases the cross section by roughly 45%. This large "k-factor" is probably mostly due to the nonrelativistic treatment of the J/ψ, in which all information about the wave function is contained in $|R(0)|^2$. One can therefore expect a similar k-factor for our reaction, so that our results for total cross sections should be considered as conservative estimates. In accord with our philosophy, we use the one-loop expression for α_s with $N_f = 4$ active flavors and $\Lambda_{QCD} = 200\ MeV$, and we take $Q^2 = m_\psi^2 + p_T^2$ as momentum scale both in α_s and in the structure functions.

In a hadronic environment, a J/ψ can probably only be identified when it decays into an e^+e^- or $\mu^+\mu^-$ pair; all our results therefore include a factor of 0.14, which is [14] the combined branching ratio for these decays. Our final state thus consists of a hard, isolated photon in one hemisphere, balanced by an e^+e^- or $\mu^+\mu^-$ pair in the opposite hemisphere, without any hadronic activity (other than the usual spectator jets resulting from the break-up of the incoming hadrons). This signal should be virtually free of any physical or instrumental backgrounds. We are now in a position to present predictions for $J/\psi + \gamma$ production at $p\bar{p}$ and ep colliders.

2. $p\overline{p}$ collisions

We begin with a discussion of $J/\psi + \gamma$ production in $p\bar{p}$ collisions. We focus on the Tevatron, which offers the largest cross sections of all existing colliders, and is expected to eventually accumulate an integrated luminosity of at least several hundred pb^{-1}. As discussed above, we require the J/ψ meson to decay into a pair of charged leptons. We then apply the following cuts, which should guarantee that the events are contained in the detectors and can be triggered upon:

$$p_T^\gamma = p_T^\psi > 5\ GeV; \tag{7a}$$

$$|y^{\gamma,e,\mu}| < 3.5. \tag{7b}$$

At present, the CDF detector can only detect muons with $|y^\mu| < 0.7$, but future upgrades, as well as the upcoming D0 detector, should provide better coverage; Eq. (7b) roughly describes the coverage of the electromagnetic calorimeters at CDF.

In Figs. 2a,b we present the transverse momentum and energy spectra of the photon and the two leptons after the cuts (7) have been applied, where we have used EHLQ1 structure functions [15]. In both figures we show the spectrum of the "harder" (denoted by 'b') and "softer" (denoted by 's') lepton separately, where the "hardness" is defined by the quantity plotted. Notice that the cut (7a) implies that at least one lepton satisfies $p_T^{l_b} > 2.5\ GeV$, $E^{l_b} > 2.9\ GeV$; together with the hard photon, this harder lepton can therefore be used to construct a trigger for this reaction. The transverse momentum and energy of the other lepton can in principle be arbitrarily small; however, Figs. 2 show that the additional cuts p_T^l, $E^l > m_\psi/2$ would not reduce the signal very much. On the other hand, it is necessary to include events where at least one lepton has less than 5 GeV transverse momentum. Due to the relatively mild cut (7b) on the rapidities of the final state particles, the energy distributions are substantially harder than the p_T spectra. Events where the whole $J/\psi + \gamma$ system undergoes a strong boost are interesting since they can yield information about the gluon densities at very small x, down to a few times 10^{-4}.

In Fig. 3a we show the rapidity distribution of the produced photon. As discussed in Sec. 1, the overall normalization of the cross section is quite uncertain. We therefore normalize these distributions by dividing by the total cross section after cuts. In order to demonstrate the sensitivity of this distribution to the shape of the gluon density function $f_{g|p}$, we show results for the EHLQ1 [15] and DO2 [16] parametrizations. These two parametrizations make quite different assumptions about the large x behaviour of $f_{g|p}$:

$$f_{g|p}(x, Q_0^2 = 5\ GeV^2) \propto x^{-1}(1 + 3.5x)(1 - x)^{5.9} \quad (EHLQ1); \tag{8a}$$

$$f_{g|p}(x, Q_0^2 = 4\ GeV^2) \propto x^{-1}(1 + 9x)(1 - x)^4 \quad (DO2). \tag{8b}$$

The harder gluon distribution function of the DO2 parametrization leads to a significantly broader rapidity distribution; when going from $y^\gamma = 0$ to $|y^\gamma| = 3$ the cross section only falls by a factor of 2.2, while the EHLQ1 gluon predicts a reduction by a factor of 2.9.[1]

The results of Fig. 3a have been obtained by integrating over p_T^γ and the rapidity of the J/ψ. It is conceivable that two parametrizations of $f_{g|p}$ which differ both in the large x and small x regions lead to similar results for the single differential cross section shown in this figure, since large photon rapidities correspond to very asymmetric initial states. Once a sufficiently large number of events has been accumulated, such ambiguities can be resolved by studying the triple differential cross section $d\sigma/(dp_T^\gamma dy^\gamma dy^\psi)$. As an example, we show in Fig. 3b this triple differential cross section as a function of p_T^γ at the symmetric point $y^\gamma = y^\psi = 0$. This cross section is directly proportional to $\left[f_{g|p}\left(x \simeq \sqrt{(2m_\psi^2 + 4(p_T^\gamma)^2)/s}\right)\right]^2$, where s is the $p\bar{p}$ centre-of-mass energy; the cut $p_T^\gamma > 5\ GeV$ then implies $x > 6 \cdot 10^{-3}$, while the cross section becomes too small to be useful if $p_T^\gamma > 15\ GeV$, i.e. $x > 0.02$, even if some $10^3 pb^{-1}$ of data can be accumulated. As mentioned above, the range of x values that can be probed can be extended by studying more asymmetric configurations; it should therefore be quite easy to distinguish between parametrizations whose small x behaviour is governed by a different (negative) power of x, like the HMRS+/- parametrizations of Ref. [17], which assume $x \cdot f_{g|p}(x) \propto x^{\pm 0.5}$.

3. *ep* collisions

We now turn to a discussion of $J/\psi + \gamma$ production at the upcoming ep collider HERA. Since in leading order this final state can only originate from a gg initial state, the observation of a sizeable signal would be an unambiguous proof for a nonvanishing gluon content of the photon. (The same is true [18] for inclusive J/ψ production in $\gamma\gamma$ collisions.)

---

[1] Note that the recent NMC analysis [3] gives $f_{g|p}(x) \propto x^{-1}(1 - x)^{5.1 \pm 0.9}$, which falls in the middle between the two parametrizations we use, but cannot rule out either of them.

In order to use Eq. (4) for the cross section calculation, one has to convolute the gluon content of the photon with the photon content of the electron:

$$f_{g|e}(x, Q^2) = \int_x^1 \frac{dz}{z} f_{\gamma|e}(z, Q^2) f_{g|\gamma}(\frac{x}{z}, Q^2), \tag{9a}$$

where

$$f_{\gamma|e}(z, Q^2) = \frac{\alpha}{\pi z}\left[1 + (1 - z)^2\right] \ln\frac{Q^2}{m_e^2}. \tag{9b}$$

We use the following cuts:

$$p_T^\gamma = p_T^\psi > 1.5\ GeV; \tag{10a}$$

$$-3.5 < y^{\gamma, e, \mu} < 3, \tag{10b}$$

where negative rapidities correspond to the proton beam direction. Notice that the cut (10a) is still sufficient to remove the contribution from reaction (3b); the cut (10b) roughly describes the acceptance of the ZEUS detector.

Notice that $f_{g|\gamma}$ is *not* constrained by a momentum sum rule; both the shape and the normalization of that function are unknown. It has recently been shown [19] that even a global fit to all existing data on F_2^γ does not yield much information on $f_{g|\gamma}$. Our results should therefore be taken as examples, not QCD predictions.

In Figs. 4a,b we show the transverse momentum and energy spectrum that result when the LAC1 parametrization [19] is used for $f_{g|\gamma}$. We see that the signal will only be useful if one lepton is allowed to have p_T below 2 GeV; on the other hand the cut (10a) and the Jacobian peak in the p_T distribution of the leptons relative to the axis of the J/ψ imply that one lepton usually does have more than 2 GeV transverse momentum. Also, due to the asymmetric nature of ep colliders, the difference between the energy distributions of Fig. 4a and the p_T distributions of Fig. 4b is even more pronounced than for $p\bar{p}$ colliders; e.g., one could impose a cut $E^\gamma > 5\ GeV$ without loosing much signal. Such a cut might be helpful since the resolution of electromagnetic calorimeters increases, and hence the relative errors on E^γ and p_T^γ shrink, with $\sqrt{E^\gamma}$.

In Fig. 5 we again compare the shape of the photon rapidity distributions as predicted by different parametrizations of photon structure functions. The present lack of data constraining $f_{g|\gamma}$ is reflected by the large differences between the three curves, corresponding to sets 1 and 3 of Ref. [19] and the older DG parametrization of Ref. [20], even though we have used a logarithmic scale for the y-axis. In Ref. [20] it was assumed that all gluons inside photons originate from radiation off quarks; in contrast, the analysis of Ref. [19] includes a truely "intrinsic" gluon inside the photon. At the input scale, the three parametrizations for $f_{g|\gamma}$ have the following functional forms:

$$f_{g|\gamma}(x, Q_0^2 = 4\ GeV^2) \propto x^{-1.34}(1 - x)^{12.6} \quad (LAC1); \tag{11a}$$

$$f_{g|\gamma}(x, Q_0^2 = 1\ GeV^2) \propto x^{5.9}(1 - x)^{0.56} \quad (LAC3); \tag{11b}$$

$$f_{g|\gamma}(x, Q_0^2 = 1\ GeV^2) \propto x^{-1.41}(1 - x)^{4.5} \quad (DG). \tag{11c}$$

Clearly, the LAC3 parametrization is rather "pathological"; however, even this extremely hard gluon distribution cannot be ruled out by data on F_2^γ alone. Fig. 5 shows that it would lead to a rapidity distribution that is much more symmetric around $y^\gamma = 0$ than the predictions of the other two parametrizations. Notice that the LAC2 gluon distribution falls even more rapidly at large x than is assumed in the LAC1 parametrization; it thus predicts even fewer events with $y^\gamma > 0$. We therefore conclude that a few dozen well measured $J/\psi + \gamma$ events at HERA would suffice to distinguish between the DG and the three LAC parametrizations, using only the *shape* of the rapidity distribution. Of course, there is no guarantee that any of these parametrizations will describe the data.

4. Summary and Conclusions

In this letter we studied the associate production of a hard, isolated photon and a J/ψ meson at $p\bar{p}$ (or pp) and ep colliders. In leading order this final state can only be produced by gluon fusion; the theoretical interpretation of any observed signal should therefore be considerably simpler than either for inclusive direct photon production or inclusive J/ψ production, where several initial states can lead to essentially the same final state. Furthermore, since we require the J/ψ to decay into a pair of charged leptons, the only final state particles with sizeable transverse momentum are leptons and photons, whose energies and momenta can be measured with high precision, so that the final state can be fully reconstructed. The cleanliness of this signal should also guarantee that instrumental backgrounds are very small.

In Table 1 we list the total production cross sections after the cuts of Eqs. (7) (for the $p\bar{p}$ case) and (10) (for ep) have been applied. We remind the reader that we used the colour singlet model to compute these cross sections; this model has been found [3] to describe kinematical distributions of inclusive J/ψ photoproduction quite well, but might underestimate the total rate by as much as a factor 3. Recall that J/ψ photoproduction at low energies is dominated by the first reaction in Eq. (2), which is related to our subprocess by crossing. If the k-factor found in Ref. [3] is indeed mostly due to the treatment of the J/ψ as a nonrelativistic $c\bar{c}$ bound state, one should expect a similar enhancement factor for our reaction. In that case, the cross section after cuts at HERA could be close to 1 pb, resulting in more than 100 events in a HERA year of 200 pb^{-1}, if the LAC parametrizations give a good description of the gluon content of the photon $f_{g|\gamma}$. Even if one does not trust this argument, and allows a theoretical error of a factor 2-3 for the prediction of total cross sections, the number of observed $J/\psi + \gamma$ events can still yield meaningful information on the overall normalization of $f_{g|\gamma}$, as demonstrated by the large differences in the entries of Table 1 corresponding to different sets of structure functions. Finally, it is worth mentioning that both initial state QCD corrections and the effects due to the nonrelativistic treatment of J/ψ will be the same for $g + g \rightarrow J/\psi + \gamma$ and $g + g \rightarrow J/\psi + g$; one can therefore use the former process to normalize the predictions for the the latter reaction, whose cross section is enhanced by a factor $15\alpha_s/16\alpha \simeq 30$. This should be possible even if the total number of $J/\psi + \gamma$ events is too small to allow a detailed study of kinematical distributions, and could simplify the analysis of inclusice J/ψ production considerably, see Eq. (1). On the other hand, the results of Table 1 and Fig. 5 indicate that the rapidity distribution of the photons produced in association with J/ψ should allow a fairly detailed analysis of the shape of $f_{g|\gamma}$ once HERA has accumulated several hundred pb^{-1} of data.

The situation at $p\bar{p}$ (or pp) colliders is quite different, since the overall normalization of the gluon density $f_{g|p}$ is given by the momentum sum rule. Furthermore, a considerable body of data that constrain $f_{g|p}$ already exists. In view of the theoretical uncertainty it is therefore unlikely that the total $J/\psi + \gamma$ rate will allow to extract meaningful new information on the *normalization* of $f_{g|p}$. However, the results of Table 1 show that already next year's Tevatron collider run, which is expected to accumulate 30 to 50 pb^{-1} of data, could yield a sufficient number of events to allow a fairly detailed measurement of the *shape* of $f_{g|p}(x)$ for $x \geq 10^{-4}$, using the normalized rapidity distributions of the photon and/or the J/ψ.

One potential drawback of $J/\psi + \gamma$ production is that one of the leptons usually has a rather small transverse momentum, less than 6 GeV at the Tevatron and less than 3 GeV at HERA. However, the second lepton, as well as the photon, are usually much harder, so that the construction of an effective trigger should still be possible. In view of the potential importance of $J/\psi + \gamma$ production as a very clean probe of gluon distribution functions we urge our experimental colleagues to make sure that these events can indeed be observed.

Acknowledgements

We thank R.J.N. Phillips for helpful discussions. One of us (C.S.K.) thanks the DESY theory group for their hospitality. The work of C.S.K. was supported by the Science and Engineering Research Council, UK.

References

[1] V. Barger and A.D. Martin, Phys. Rev. **D31**, 1051 (1985).

[2] T. Weiler, Phys. Rev. Lett. **44**, 304 (1980); A.D. Martin, C.-K. Ng and W.J. Stirling, Phys. Lett. **B191**, 200 (1987); Z. Kunszt, Phys. Lett. **B207**, 103 (1988); J. Abraham, Phys. Lett. **B240**, 224 (1990).

[3] NMC collab., D. Allasia et al., Phys. Lett. **B258**, 493 (1991).

[4] Z. Kunszt and W.J. Stirling, Phys. Lett. **B217**, 53 (1989).

[5] E. Witten, Nucl. Phys. **B120**, 189 (1977).

[6] R.S. Fletcher, F. Halzen and R.W. Robinett, Phys. Lett. **B225**, 176 (1989).

[7] J. Abraham, NIKHEF preprint H-91-02; R.S. Fletcher, F. Halzen, S. Keller and W.H. Smith, Univ. Wisconsin preprint MAD/PH/633 (1991).

[8] AMY collab., R. Tanaka et al., KEK preprint 91-14.

[9] A.D. Martin, R.G. Roberts and W.J. Stirling, Phys. Rev. **D37**, 1161 (1988).

[10] J. Owens, Rev. Mod. Phys. **59**, 465 (1987).

[11] A.C. Bawa, M. Krawczyk and W.J. Stirling, Z. Phys. **C50**, 293 (1991); A.C. Bawa and M. Krawczyk, Phys. Lett. **B262**, 492 (1991).

[12] R.S. Fletcher, F. Halzen and E. Zas, Phys. Lett. **B221**, 40~~9~~3 (1989); M. Drees and C.S. Kim, DESY preprint 91-039, to appear in Z. Phys. C.

[13] E.L. Berger and D. Jones, Phys. Rev. **D23**, 1521 (1981); R. Baier and R. Rückl, Z. Phys. **C19**, 251 (1983); R. Gastmans, W. Troost and T.T. Wu, Phys. Lett. **B184**, 257 (1987).

[14] Particle Data Group, Phys. Lett. **B239**, 1 (1990).

[15] E.J. Eichten, I. Hinchliffe, K.O. Lane and C. Quigg, Rev. Mod. Phys. **56**, 579 (1984).

[16] D.W. Duke and J. Owens, Phys. Rev. **D30**, 49 (1984).

[17] P.N. Harriman, A.D. Martin, R.G. Roberts and W.J. Stirling, Phys. Lett. **B243**, 421 (1990).

[18] M. Drees and R.M. Godbole, Nucl. Phys. **B339**, 355 (1990).

[19] H. Abramowicz, K. Charchula and A. Levy, DESY preprint 91-069.

[20] M. Drees and K. Grassie, Z. Phys. **C28**, 451 (1985).

Table Captions

Table 1 : The integrated cross sections $\sigma(g+g \to J/\psi(\to l+\bar{l})+\gamma)$ with $p_T^\gamma > 1.5$ GeV, $-3.5 < y^{\gamma,l} < 3$ at HERA (ep, $\sqrt{s} = 314$ GeV), and $p_T^\gamma > 5$ GeV, $|y^{\gamma,l}| < 3.5$ at TEVATRON ($p\bar{p}$, $\sqrt{s} = 1800$ GeV) using the various gluon structure functions for $f_{g/\gamma}$ and $f_{g/p}$.

Structure Function	$\sigma(J/\psi(\to l+\bar{l})+\gamma)$ (pb)
ep (DG⊗EHLQ1)	0.08
ep (LAC1⊗EHLQ1)	0.34
ep (LAC3⊗EHLQ1)	0.28
$p\bar{p}$ (EHLQ1⊗EHLQ1)	30.8
$p\bar{p}$ (DO2⊗DO2)	27.5

Figure Captions

Fig. 1 Feynman diagram for $g + g \to J/\psi + \gamma$; the diagram with crossed gluon lines has to be added.

Fig. 2 The transverse momentum (a) and energy (b) spectrum of the photon and the two leptons from $J/\psi + \gamma$ production at the Tevatron collider with subsequent $J/\psi \to e^+e^-, \mu^+\mu^-$ decay, after the cuts of Eq. (7) have been applied. The subscripts "b" and "s" refer to the lepton with the bigger and smaller p_T (in a) or energy (in b), respectively.

Fig. 3 The normalized rapidity distribution (a) and transverse momentum spectrum at the point $y^\gamma = y^\psi = 0$ (b) of the photon from $J/\psi + \gamma$ production at the Tevatron collider. Results for different parmetrizations of the gluon content of the proton are compared: solid curves - set 1 of Ref. [15]; dashed curves - set 2 of Ref. [16].

Fig. 4 The transverse momentum (a) and energy (b) spectrum of the photon and the two leptons from $J/\psi + \gamma$ production at HERA with subsequent $J/\psi \to e^+e^-, \mu^+\mu^-$ decay, after the cuts of Eqs. (10) have been applied. The meaning of the subscripts "b" and "s" is as in Fig. 2.

Fig. 5 The normalized rapidity distribution of the photon from $J/\psi + \gamma$ production at HERA. The solid, short dashed and long dashed curves have been obtained using the parametrizations of Ref. [20] and sets 1 and 3 of Ref. [19], respectively, for the gluon content of the photon.

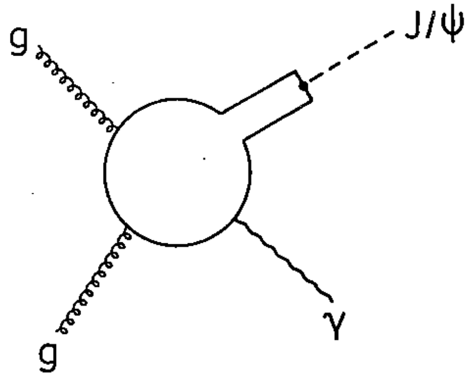

Fig. 1

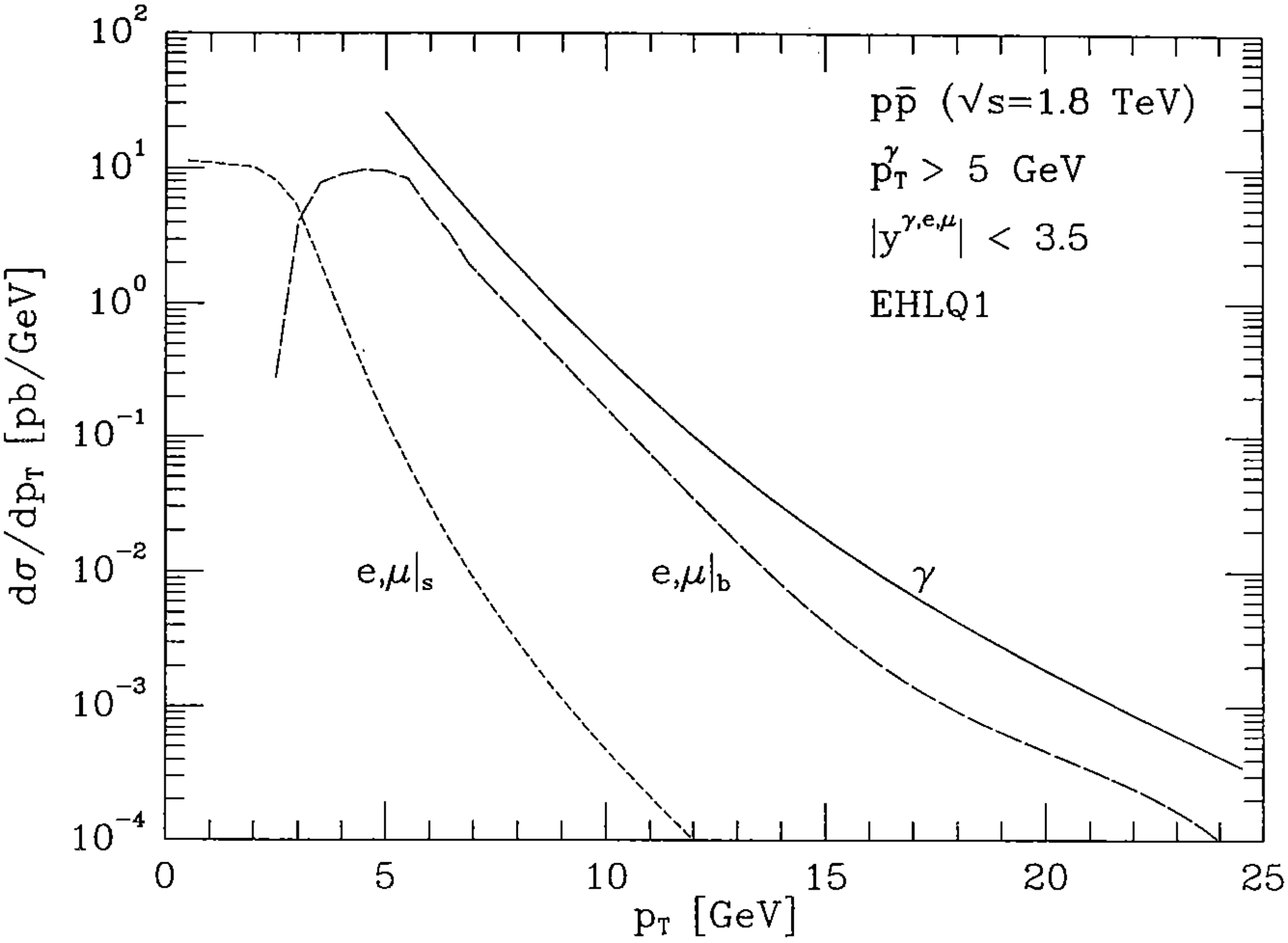
10^2
10^1
10^0
10^-1
10^-2
10^-3
10^-4
dσ/dp_T [pb/GeV]
pp̄ (√s=1.8 TeV)
p_T^γ > 5 GeV
|y^{γ,e,μ}| < 3.5
EHLQ1
e,μ|_s
e,μ|_b
γ
0
5
10
15
20
25
p_T [GeV]

Fig. 2a

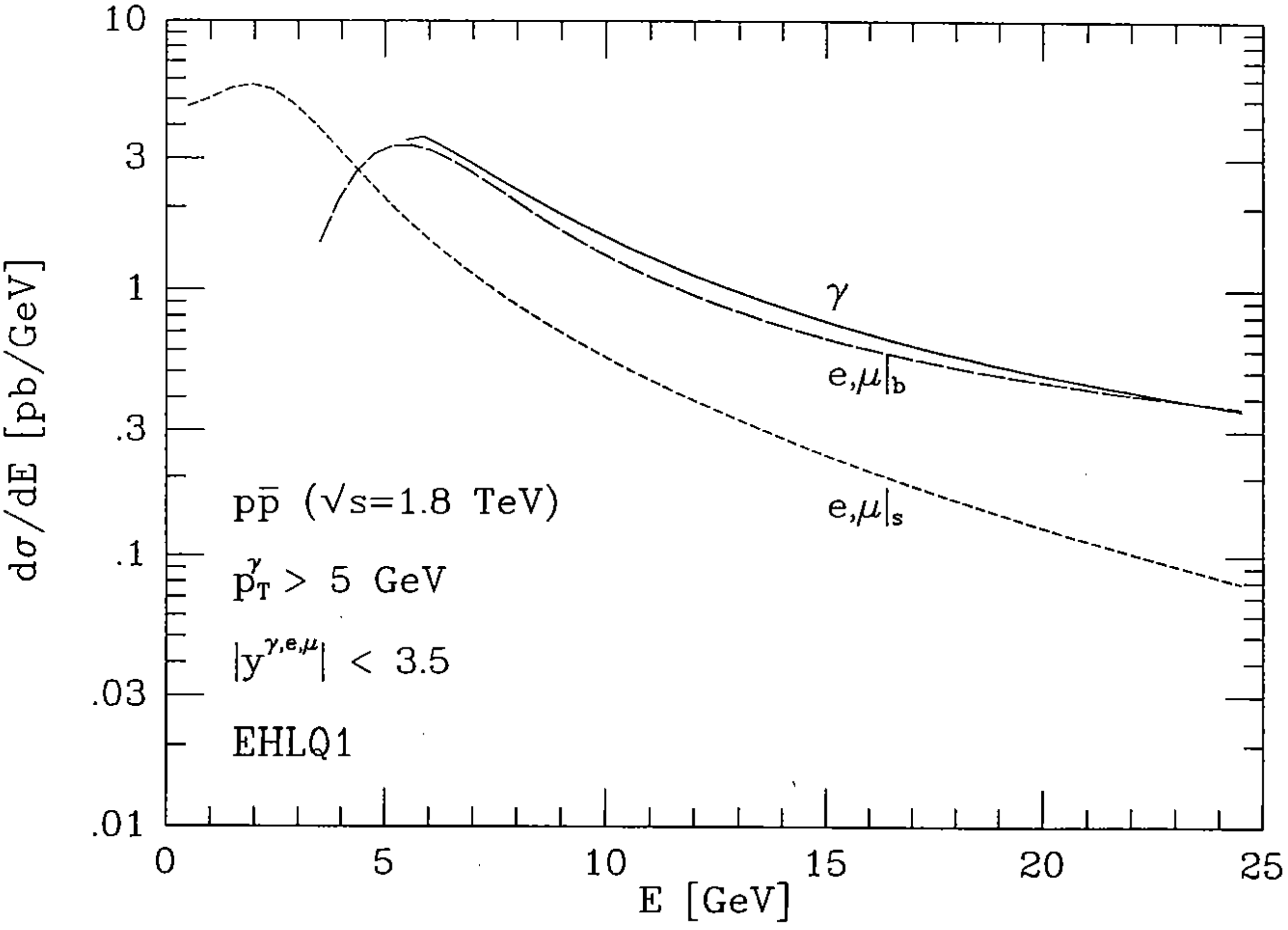
10
3
1
.3
.1
.03
.01
dσ/dE [pb/GeV]
γ
e,μ|_b
e,μ|_s
pp̄ (√s=1.8 TeV)
p_T^γ > 5 GeV
|y^{γ,e,μ}| < 3.5
EHLQ1
0
5
10
15
20
25
E [GeV]

Fig. 2b

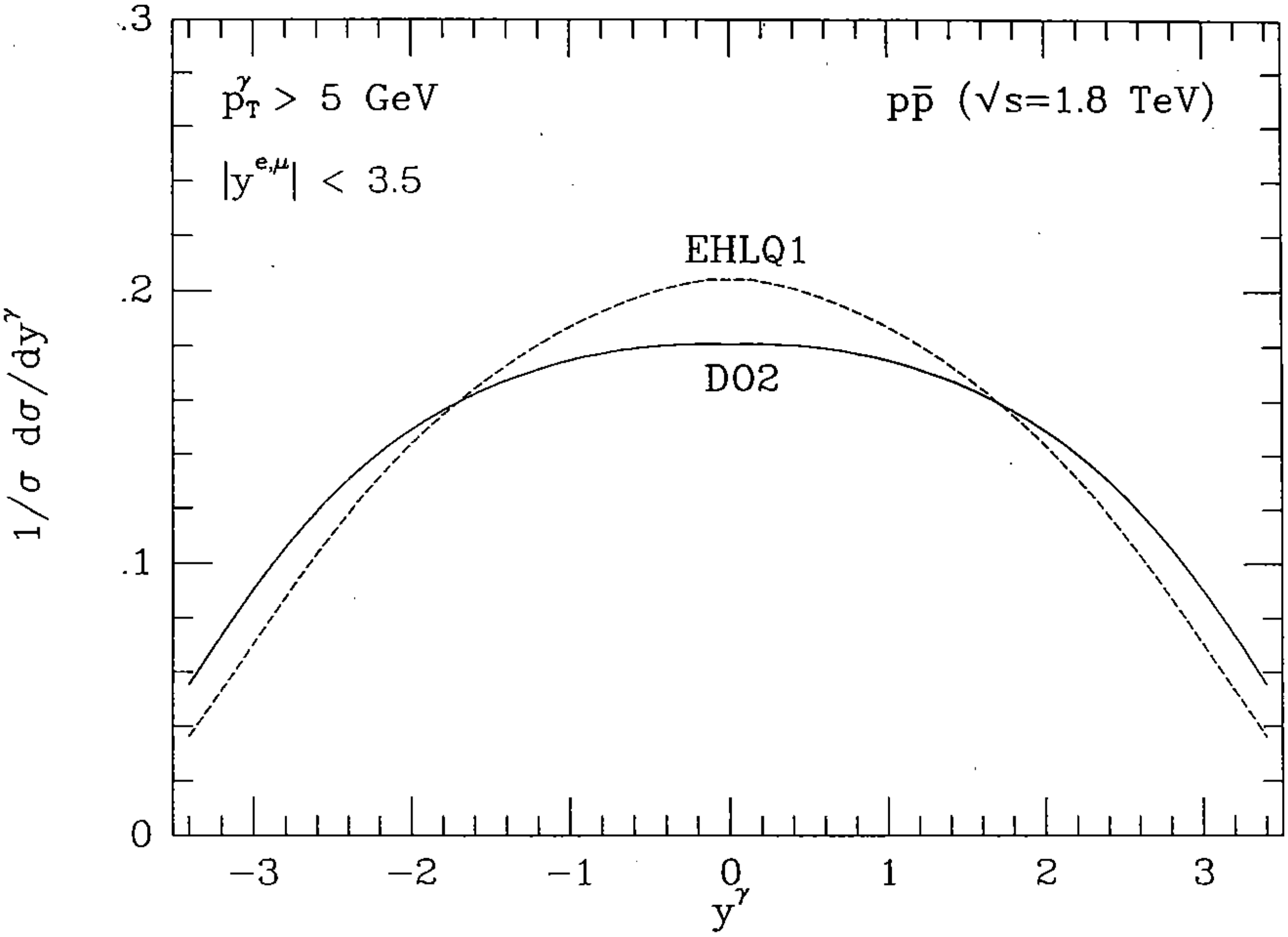
$p_T^\gamma > 5$ GeV
$|y^{e,\mu}| < 3.5$
$p\bar{p}$ ($\sqrt{s}$=1.8 TeV)
EHLQ1
DO2
$1/\sigma\, d\sigma/dy^\gamma$
y^γ
.3
.2
.1
0
−3
−2
−1
0
1
2
3

Fig. 3a

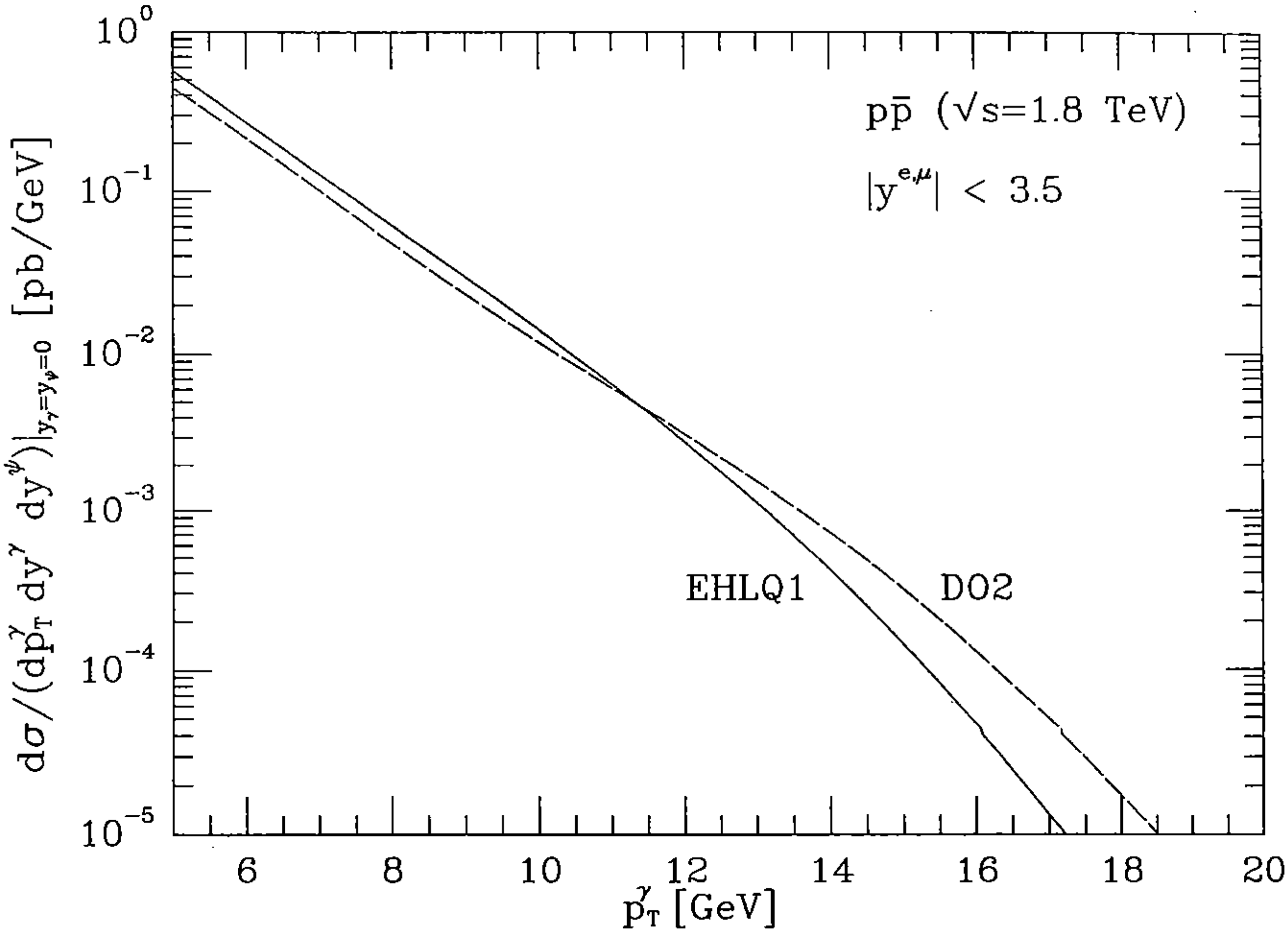
$p\bar{p}$ ($\sqrt{s}$=1.8 TeV)
$|y^{e,\mu}| < 3.5$
EHLQ1
DO2
$d\sigma/(dp_T^\gamma\, dy^\gamma\, dy^\psi)|_{y_\gamma=y_\psi=0}$ [pb/GeV]
p_T^γ [GeV]
10^0
10^{-1}
10^{-2}
10^{-3}
10^{-4}
10^{-5}
6
8
10
12
14
16
18
20

Fig. 3b

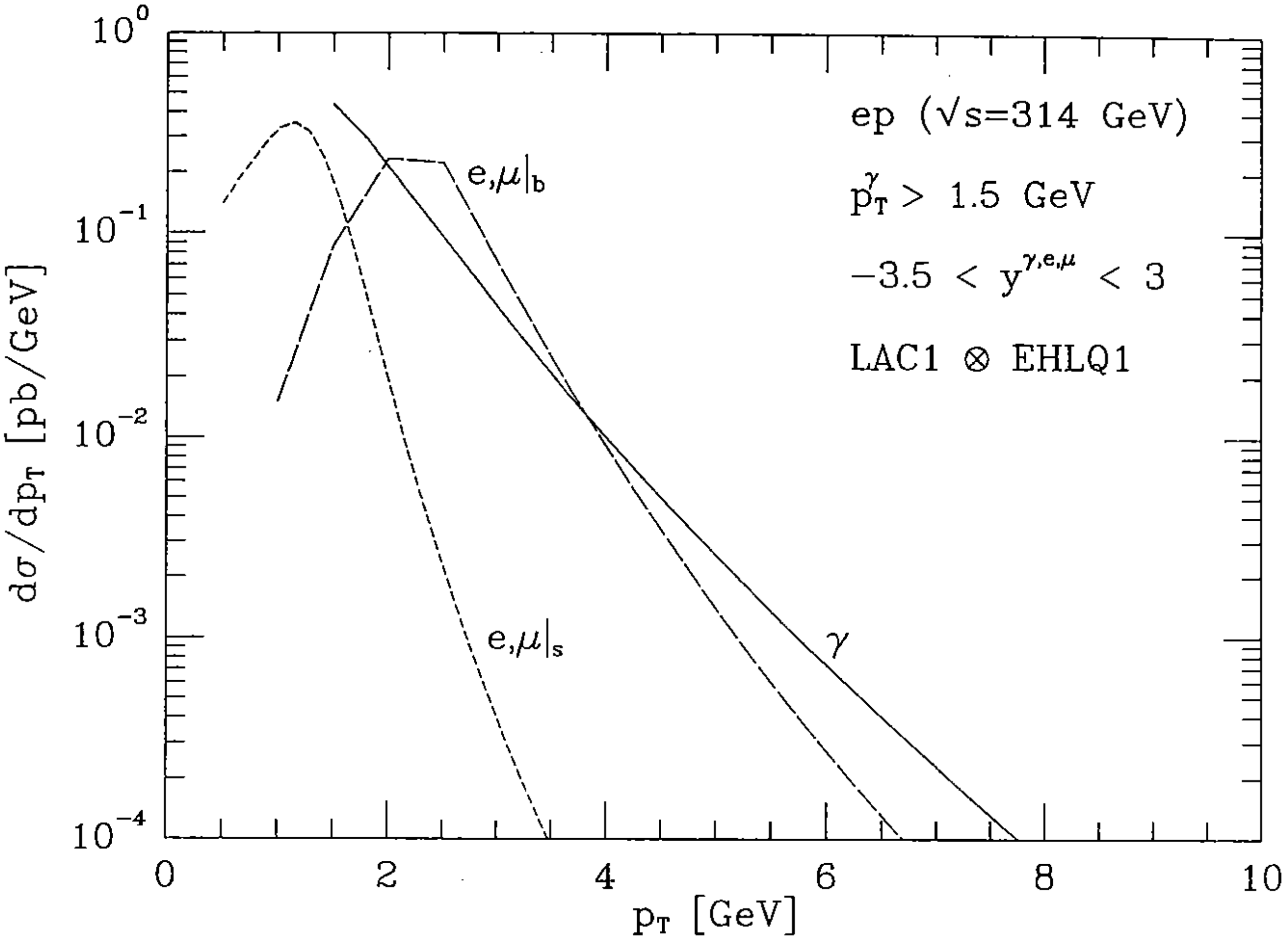
ep ($\sqrt{s}$=314 GeV)
$p_T^\gamma > 1.5$ GeV
$-3.5 < y^{\gamma,e,\mu} < 3$
LAC1 ⊗ EHLQ1
$e,\mu|_b$
$e,\mu|_s$
γ
$d\sigma/dp_T$ [pb/GeV]
p_T [GeV]
10^0
10^{-1}
10^{-2}
10^{-3}
10^{-4}
0
2
4
6
8
10

Fig. 4a

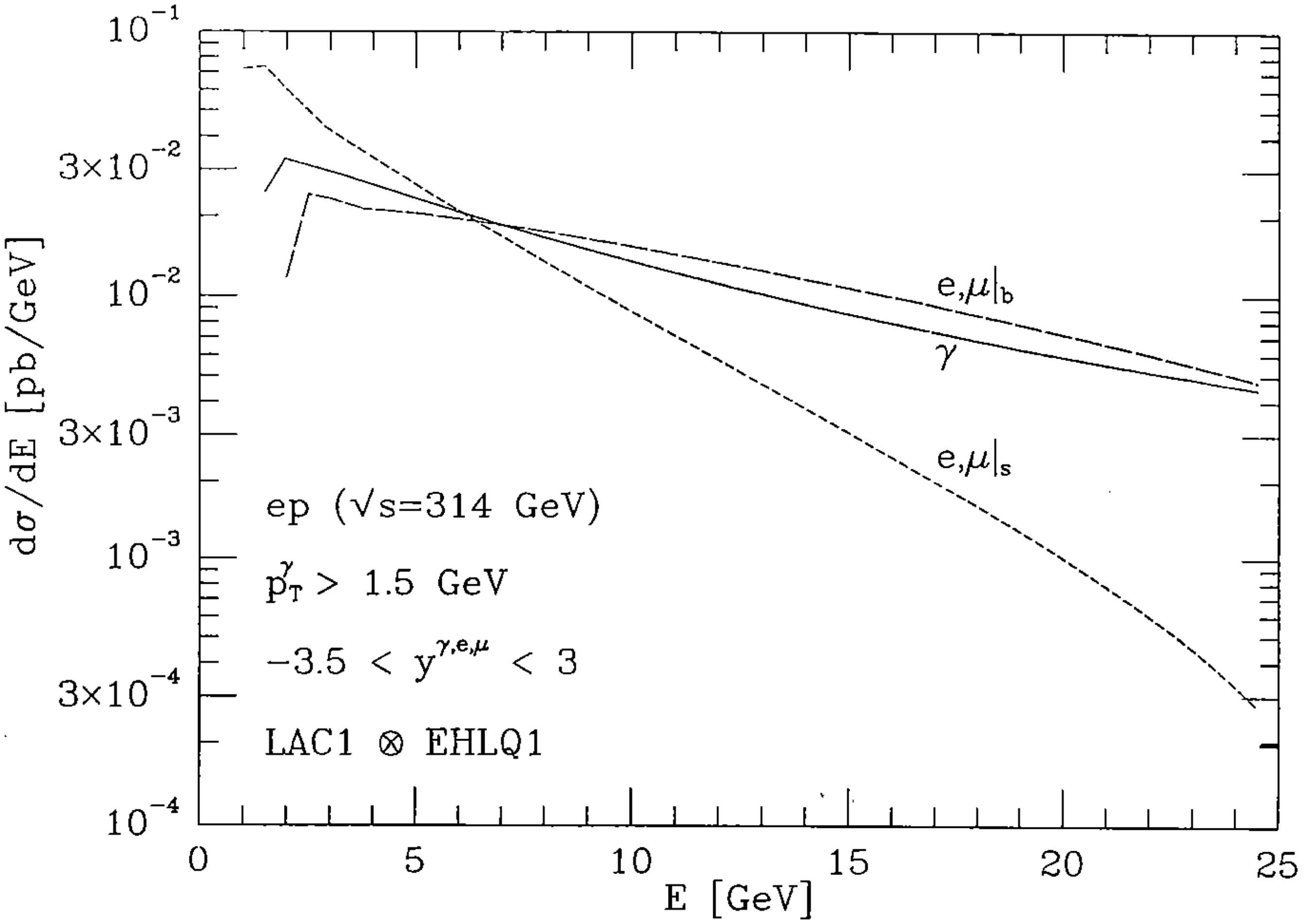
$e,\mu|_b$
γ
$e,\mu|_s$
ep ($\sqrt{s}$=314 GeV)
$p_T^\gamma > 1.5$ GeV
$-3.5 < y^{\gamma,e,\mu} < 3$
LAC1 ⊗ EHLQ1
$d\sigma/dE$ [pb/GeV]
E [GeV]
10^{-1}
3×10^{-2}
10^{-2}
3×10^{-3}
10^{-3}
3×10^{-4}
10^{-4}
0
5
10
15
20
25

Fig. 4b

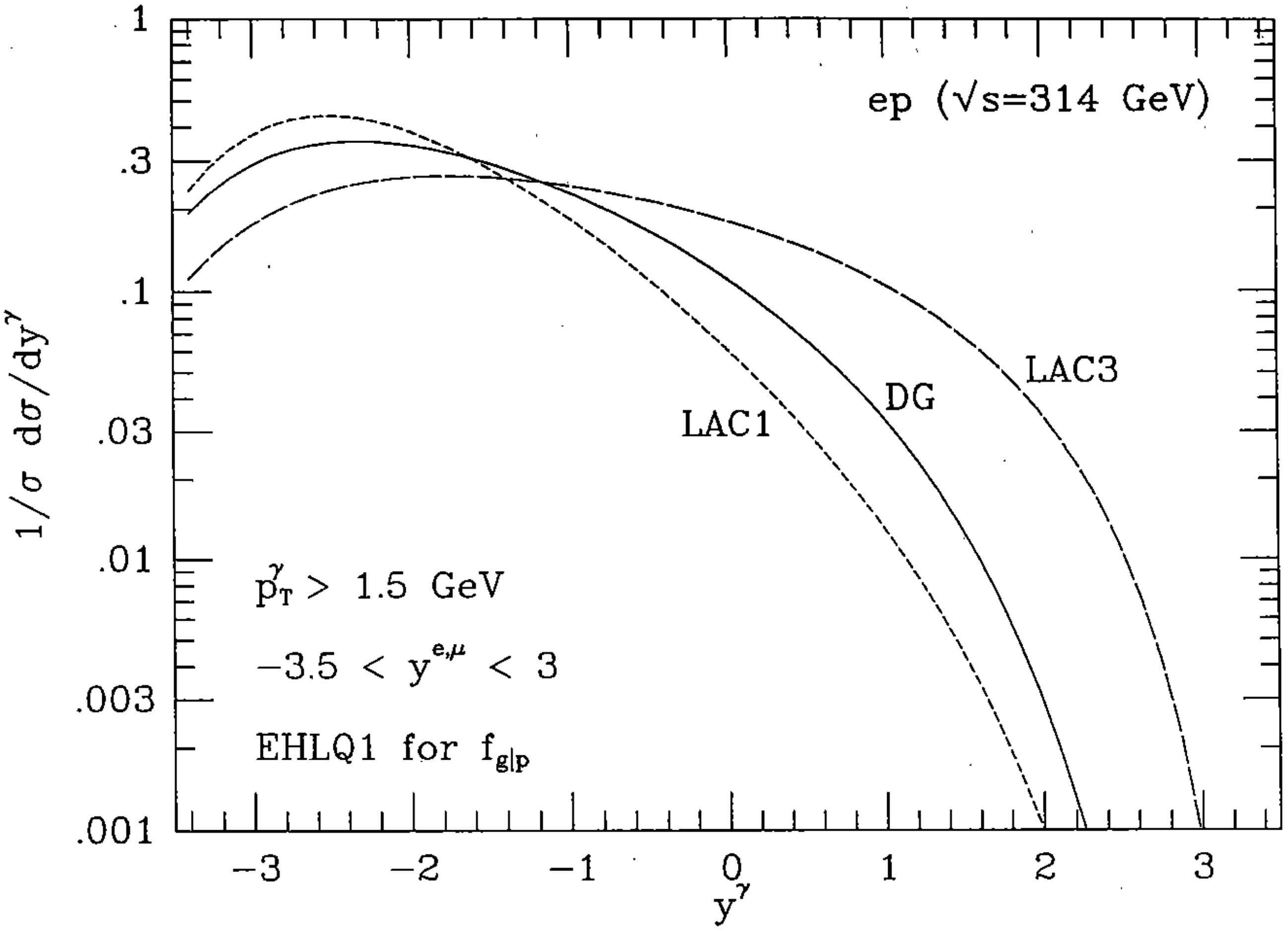
ep ($\sqrt{s}$=314 GeV)
$1/\sigma\ d\sigma/dy^{\gamma}$
1
.3
.1
.03
.01
.003
.001
LAC3
DG
LAC1
$p_T^{\gamma} > 1.5$ GeV
$-3.5 < y^{e,\mu} < 3$
EHLQ1 for $f_{g|p}$
−3
−2
−1
0
1
2
3
y^{γ}

Fig. 5